

Received May 6, 2020, accepted May 18, 2020, date of publication June 15, 2020, date of current version June 26, 2020.

Digital Object Identifier 10.1109/ACCESS.2020.3002433

# Characterization and Design of Wideband Penta- and Hepta-Resonance SIW Elliptical Cavity-Backed Slot Antennas

LEI XIANG<sup>1</sup>, YAN ZHANG<sup>1</sup>, (Member, IEEE),  
YINGRUI YU<sup>1</sup>, (Graduate Student Member, IEEE),  
AND WEI HONG<sup>1</sup>, (Fellow, IEEE)

State Key Laboratory of Millimeter Waves, School of Information Science and Engineering, Southeast University, Nanjing 210096, China

Corresponding author: Yan Zhang (yanzhang\_ise@seu.edu.cn)

This work was supported in part by the National Natural Science Foundation of China (NSFC) under Grant 61971132 and Grant 61861136002, and in part by the Fundamental Research Funds for the Central Universities.

**ABSTRACT** Substrate integrated waveguide (SIW) elliptical cavity-backed slot antennas (CBSAs) with either penta- or hepta-resonance are characterized and designed for wideband performance in this paper. First, the resonant behavior of the elliptical cavity is explored. Then the SIW CBSA with penta-resonance is designed by introducing a cross-shaped slot and a pair of unbalanced shorting vias into the cavity to excite two additional odd- and even- half degenerate quasi-TM<sub>110</sub> modes, besides other three modes of half quasi-TM<sub>010</sub>, and odd- and even- quasi-TM<sub>110</sub>. Further, by adding another pair of unbalanced shorting vias, two extra higher-order modes, i.e., odd- and even- quasi-TM<sub>210</sub> modes are successfully introduced to design a hepta-resonance antenna. The corresponding mode analysis and design guidelines are discussed in detail. Two prototypes are fabricated and measured at X-band, exhibiting the measured bandwidths of 21.8% and 22.7%, respectively. Measured results agree well with simulations, thus validating the design concept.

**INDEX TERMS** Elliptical cavity-backed slot antenna, mode analysis, wideband applications, substrate integrated waveguide (SIW).

## I. INTRODUCTION

Recently, low profile antenna with wideband performance plays a crucial role during the development of high-capacity wireless communication networks. For instance, wireless applications operating at X-band, including marine radar, satellite communication and motion detection, are in great demand for planar wideband antennas [1]–[3]. Substrate integrated waveguide (SIW) cavity-backed slot antennas (CBSAs) have been extensively investigated because they own excellent characteristics of low profile, high efficiency, easy fabrication, low cost, and convenient integration with planar circuits [4]–[27]. However, one evident drawback of conventional SIW CBSA is the narrow operating bandwidth (approximately only 1.7%) due to both the high quality factor and single-mode resonance of the cavity [4].

To alleviate this problem, several methods have been proposed to enhance the bandwidth of SIW CBSAs, which

The associate editor coordinating the review of this manuscript and approving it for publication was Yasar Amin<sup>1</sup>.

can be generally categorized into three types. The first type is to use multiple resonant cavity modes jointly to enlarge the bandwidth [5]–[14]. Two hybrid cavity modes are excited through a non-resonant rectangular slot, achieving a relative bandwidth of 6.3% in [5]. In [6], the rectangular slot is replaced with a bow-tie-shaped slot and the bandwidth is enhanced to 9.4%. Using a triangular complementary split-ring slot, the SIW CBSA realizes a bandwidth of 16.7% in [8]. Several broadband SIW CBSAs are represented by using coupled half-mode/quarter-mode/eighth-mode of a split SIW cavity [10]–[12]. In [13] and [14], shorting vias are introduced into the SIW cavity to generate triple- and quad-resonance, and quad- and penta-resonance, achieving bandwidths of 15.2% and 17.5%, 20.0% and 20.8%, respectively. However, the number of used combined cavity modes is no more than five, which limits the bandwidth. The second type is to combine the cavity mode with the radiating slot mode to acquire a wide bandwidth [15]–[17]. Although the antenna in [15] utilizes the higher-order resonant modes (TE<sub>130</sub>, TE<sub>310</sub>, TE<sub>330</sub>) which yields the wide fractional

bandwidth ( $>26\%$ ), it occupies a much larger SIW cavity size. The third type is to load a patch onto the cavity through a slot, combining the cavity mode with additional resonant patch mode [18], [19]. In [18], a cavity mode  $TE_{210}$  and an additional patch mode are excited to achieve a bandwidth of 15%, which, in fact, is still narrow. Moreover, the published SIW CBSAs are mainly implemented with the ordinary rectangular cavities [4]–[19], circular cavities [20]–[25], triangle cavity [26], and hexagonal cavity [27]. To this end, novel broadband antenna topologies need to be further explored to utilize more cavity modes, aiming to exhibit a wider bandwidth to satisfy the increasing requirement from the modern communication system.

In this paper, different from the aforementioned SIW CBSAs based on conventional cavities [4]–[27], a study on exploring and exploiting multiple resonant modes in an SIW elliptical cavity is put forward for wideband SIW CBSAs design. Besides, only the cavity modes are utilized to realize a wide bandwidth, thus possessing design simplicity and convenience. A constructive point of view on the elliptical cavity is that its flexible control ability of resonant modes through the axial ratio  $k$  (the ratio between the major and minor axes of the ellipse), providing an extra design freedom [28]. More importantly, the characterization analysis for the eigenmodes in resonant cavity is thoroughly conducted according to the peculiarity of elliptical cavity, which is very essential and insightful for the CBSAs design and implementation. First, a penta-resonance antenna with a bandwidth of 21.8% is obtained with the aid of a cross-shaped slot and two unbalanced shorting vias, successfully generating five resonant modes in the elliptical cavity. Further, by introducing another pair of unbalanced shorting vias, a hepta-resonance antenna is acquired with two additional resonant modes, together with a wider bandwidth of 22.7%. The prototyped antennas are fabricated with conventional single-layer printed circuit board (PCB) process, having features of low cost and mass production.

## II. CHARACTERIZATION OF ELLIPTICAL CAVITY

To characterize the resonant behavior in an elliptical cavity, the first four resonant modes have been simulated and compared with their counterparts in a circular cavity, which are obtained through full wave simulations using the ANSYS High-Frequency Structure Simulator (HFSS). As discussed in [29], conventionally it is difficult to name the resonant modes in an elliptical cavity, and an alternative method proposed in this paper for naming the modes in an elliptical cavity is to compare them with their counterparts in a circular cavity. As shown in Figs. 1(a)–(d), the first four resonant modes in the circular cavity are  $TM_{010}$  mode,  $TM_{110}$  mode, degenerate  $TM_{110}$  mode, and  $TM_{210}$  mode, respectively. It should be noted that both the circular and elliptical cavities are analyzed with a very small thickness ( $\sim 0.016\lambda$ ) as an SIW cavity usually has, which means there is no variation of E-field along  $z$ -axis. When observing the E-field distributions in the elliptical cavity with  $k = 1.3$ , as illustrated in Figs. 2(a)–(d),

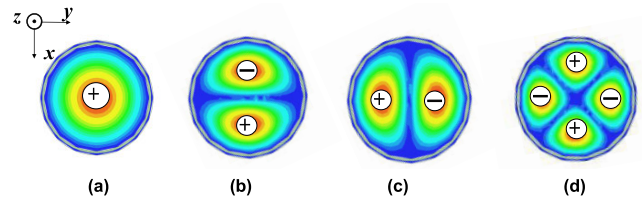


**FIGURE 1.** E-field distributions of the first four resonant modes in a low-profile circular cavity. (a)  $TM_{010}$  mode, (b)  $TM_{110}$  mode, (c) degenerate  $TM_{110}$  mode, (d)  $TM_{210}$  mode.

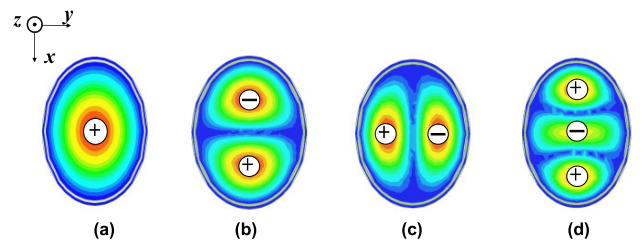


**FIGURE 2.** E-field distributions of the first four resonant modes in a low-profile elliptical cavity. (a) quasi- $TM_{010}$  mode, (b) quasi- $TM_{110}$  mode, (c) degenerate quasi- $TM_{110}$  mode, (d) quasi- $TM_{210}$  mode.

we find that the resonant modes in the elliptical cavity are quite similar to their counterparts in the circular cavity (a particular elliptical cavity with  $k = 1$ ). Herein, according to the observed similarities, the first four resonant modes in the elliptical cavity can be named as quasi- $TM_{010}$  mode, quasi- $TM_{110}$  mode, degenerate quasi- $TM_{110}$  mode, and quasi- $TM_{210}$  mode, respectively, for convenience. The similarities between the elliptical and the circular cavities can pave the way using elliptical cavity for multi-mode CBSA design, and additionally, these resonant modes can be adjusted flexibly in terms of resonant frequencies, by tuning both the absolute size and the axial ratio  $k$  of the elliptical cavity. As displayed in Fig. 3, the normalized resonant frequencies of the first four modes in the elliptical cavity are plotted with  $k$  varying from 1.1 to 1.6. It can be seen that  $k$  influences obviously the frequency distribution of each resonant mode. If  $k$  is smaller than 1.2, the quasi- $TM_{110}$  mode and the degenerate quasi- $TM_{110}$  mode will be merged to each other and it is difficult to generate the corresponding odd- and even- modes. Besides, the bandwidth is narrow because of the adjacent distance between the degenerate quasi- $TM_{110}$  mode and the quasi- $TM_{210}$  mode if  $k$  is too large, i.e., 1.5 or even larger.

Thereby, choosing  $k$  at the approximate range of 1.3–1.4 for the frequency separation and optimal bandwidth. Furthermore, it is worth noticing that here  $k$  is served as a relative and independent value of operating frequency, which implies the cavity as well as the corresponding CBSA can be flexibly implemented to operate at any desired frequency band.

## III. DESIGN OF SIW ELLIPTICAL CBSAS

### A. PENTA-MODE SIW ELLIPTICAL CBSA

First, a penta-resonance SIW elliptical CBSA is designed by implementing a cross-shaped slot and a pair of unbalanced

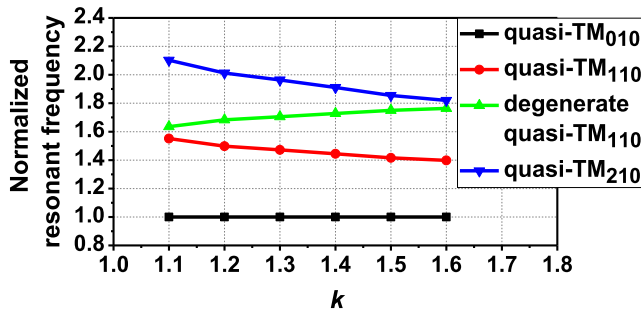


FIGURE 3. The relationship between  $k$  and the normalized resonant frequencies of the first four modes in the elliptical cavity.

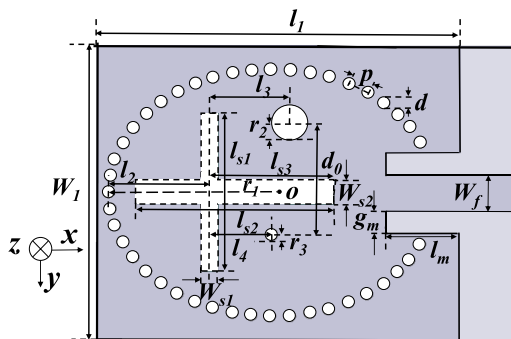


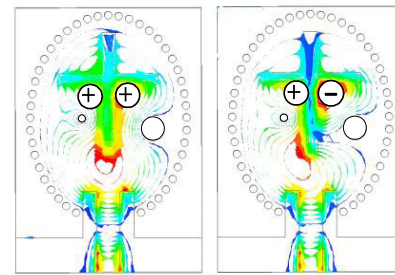
FIGURE 4. Geometry of the proposed penta-mode SIW elliptical CBSA.

TABLE 1. Dimension of the proposed penta-mode SIW elliptical CBSA.

Parameters	$l_1$	$l_2$	$l_3$	$l_4$	$l_{s1}$
Values/mm	31.0	8.64	6.79	5.33	13.4
Parameters	$l_{s2}$	$l_{s3}$	$l_m$	$w_1$	$w_{s1}$
Values/mm	16.8	10.56	6.3	25.0	1.4
Parameters	$w_{s2}$	$w_f$	$d_0$	$r_1$	$r_2$
Values/mm	1.93	3.1	9.53	14.0	1.5
Parameters	$r_3$	$g_m$	$d$	$p$	
Values/mm	0.49	1.9	1.0	1.4	

shorting vias into the elliptical cavity to generate the half quasi-TM<sub>010</sub> mode, the odd- and even-modes of quasi-TM<sub>110</sub>, and the odd- and even-modes of half degenerate quasi-TM<sub>110</sub>, which are corresponding to the aforementioned first three resonant modes of the original elliptical cavity. The geometry of the penta-mode antenna is shown in Fig. 4, and its size is determined to operate at X-band with  $k = 1.3$ . The SIW elliptical cavity is fulfilled in a substrate by arranging metallic vias along an elliptical curve. The cavity is fed through a  $50 - \Omega$  microstrip line printed on the top copper layer, and a cross-shaped slot with different widths is etched on the bottom copper layer of the cavity. Two shorting vias with different radius are placed at the opposite sides referring to the longitude slot (along  $x$ -axis). Table 1 exhibits all dimensions of the proposed penta-mode SIW elliptical CBSA.

The simulated E-field distributions of the penta-mode antenna are represented in Figs. 5(a)-(e), which are in

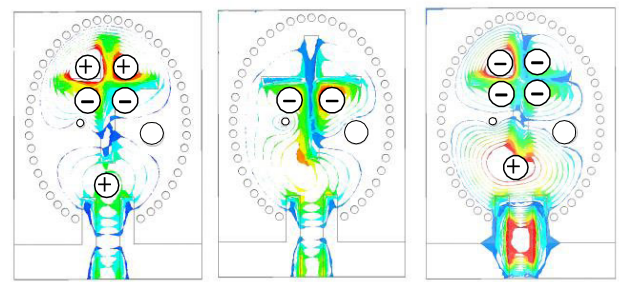


9.03 GHz

9.60 GHz

(a)

(b)



10.05 GHz

10.59 GHz

10.88 GHz

(c)

(d)

(e)

FIGURE 5. E-field distributions in the penta-mode SIW elliptical CBSA. (a) half quasi-TM<sub>010</sub> mode, (b) odd half degenerate quasi-TM<sub>110</sub> mode, (c) odd quasi-TM<sub>110</sub> mode, (d) even half degenerate quasi-TM<sub>110</sub> mode, (e) even quasi-TM<sub>110</sub> mode.

sequence regarding to half quasi-TM<sub>010</sub> mode at 9.03 GHz, odd half degenerate quasi-TM<sub>110</sub> mode at 9.60 GHz, odd quasi-TM<sub>110</sub> mode at 10.05 GHz, even half degenerate quasi-TM<sub>110</sub> mode at 10.59 GHz and even quasi-TM<sub>110</sub> mode at 10.88 GHz. The positive and negative signs inserted in Fig. 5 indicate the phases of sub regions divided by the cross-shaped slot, which are helpful to recognize the modes. As can be seen, five resonant modes are successfully generated in the proposed elliptical cavity, comparing with the quad-mode rectangular CBSA [14] in which the even half-TE<sub>120</sub> mode has not been effectively generated.

To further understand the generation of resonant modes, the design procedure is described as follows: 1) Design of the SIW elliptical cavity: including both the absolute size and  $k$ . As discussed in above, it can benefit from choosing  $k$  at the range of 1.3-1.4 that the resonant frequency of each mode can be separated sufficiently to result in a wide bandwidth; 2) Design of the cross-shaped slot: placing the latitude slot (along  $y$ -axis) at the place of the maximum E-field intensity of the quasi-TM<sub>110</sub> mode, which can introduce a discontinuity and excite the odd- and even- quasi-TM<sub>110</sub> modes with the half quasi-TM<sub>010</sub> mode [13]. Then placing the longitude slot at the place of the minimum E-field intensity of the half degenerate quasi-TM<sub>110</sub> mode to assist the generation of its odd- and even- modes with less effect on the original E-field distributions. Fig. 6 (a) depicts the generated conventional tri-mode resonance excited by the cross-shaped slot. The initial length of each slot can be chosen

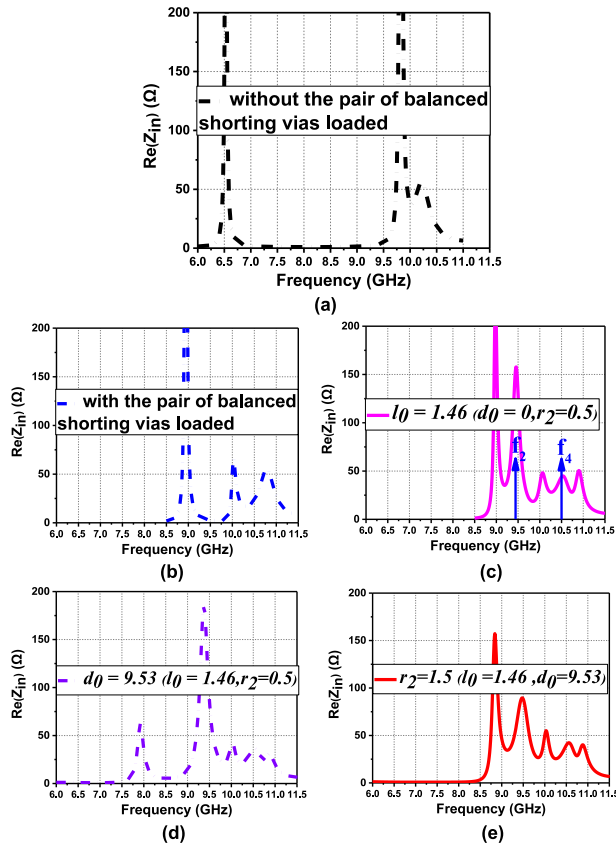


**FIGURE 6.** Simulated input resistance of the penta-mode antenna with varying values for the parameters of the pair of shorting vias. (a) without the pair of balanced shorting vias loaded, (b) with the pair of balanced shorting vias loaded, (c) the relative offset  $l_0$  along x-axis, (d) the relative offset  $d_0$  along y-axis, (e) the radius  $r_2$  of one of the shorting vias. (unit: mm).

as a half wavelength at the central frequency of the operating band, i.e., 15mm @ 10 GHz, and later both the length and the width are further optimized for impedance matching. Noting that both the latitude and the longitude slots are essentially contributing as radiators simultaneously; 3) Design of the unbalanced shorting vias: similar with the method in [14], the two balanced loaded vias are introduced firstly at the place of the minimum E-field intensity of the odd- and even-quasi-TM<sub>10</sub> modes to keep their E-field distributions almost unchanged and meanwhile shift up the resonant frequency of the half quasi-TM<sub>010</sub> mode as presented in Fig. 6 (b). Second, introducing a relative offset along x-axis between the two shorting vias, as  $l_0 = l_3 - l_4$ , to provide a perturbation for exciting the additional odd- and even- half degenerate quasi-TM<sub>10</sub> modes as shown in Fig. 6 (c). Finally, introducing another relative offset along y-axis between the two shorting vias, as  $d_0$ , and tuning the radius of two shorting vias to adjust the input resistance mainly for the first resonant mode to achieve the best impedance match performance and desired bandwidth, as illustrated in Fig. 6 (d) and (e). To be more concrete, Fig. 7 describes further the generation of the odd- and even- half degenerate quasi-TM<sub>10</sub> modes. It can be observed that the odd- and even- half degenerate quasi-TM<sub>10</sub> modes are generated with the increasing of the offset  $l_0$  along x-axis,

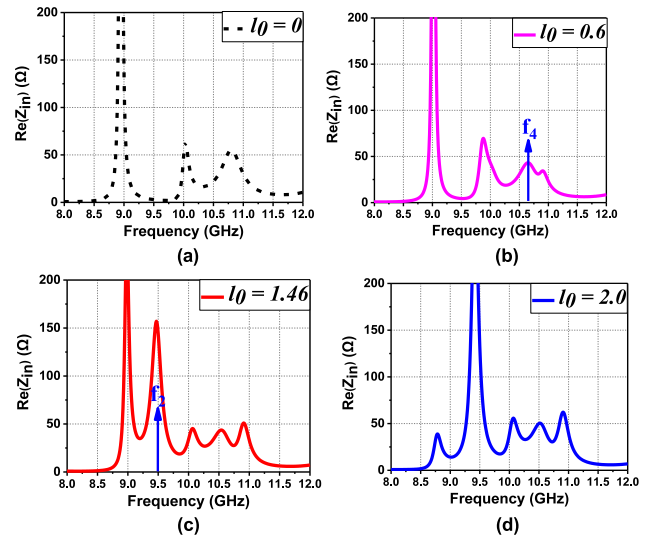


**FIGURE 7.** Simulated input resistance of the penta-mode antenna with varying value of the offset  $l_0$  between the two vias. (a)  $l_0 = 0$ , (b)  $l_0 = 0.6$ , (c)  $l_0 = 1.46$ , (d)  $l_0 = 2.0$ .

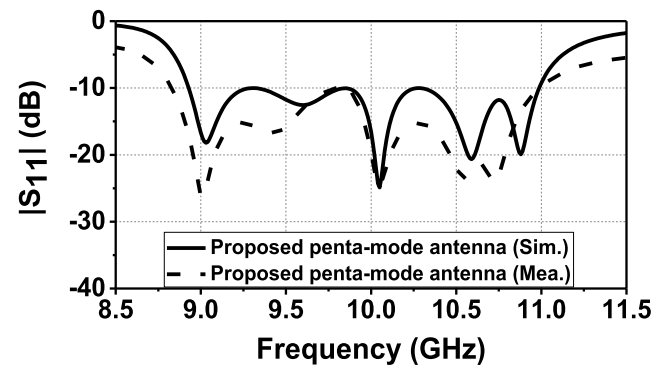


**FIGURE 8.** Measured reflection coefficient compared with the simulated results.

and  $l_0 = 1.46$  is chosen to acquire an optimal resonance. The simulated and measured S-parameter of the proposed penta-mode SIW elliptical CBSA are plotted in Fig. 8, and the measured impedance bandwidth is 21.8% (8.83–10.99 GHz).

**B. HEPTA-MODE SIW ELLIPTICAL CBSA**

To further improve the operating bandwidth, a hepta-resonance SIW elliptical CBSA is developed based on the penta-resonance CBSA, by further introducing another pair of unbalanced shorting vias into the elliptical cavity, as displayed in Fig. 9. The elliptical cavity is set with  $k = 1.4$ . Hence, the additional odd- and even-modes of quasi-TM<sub>210</sub> are successfully excited to realize the desired hepta-resonance, thus utilizing all the aforementioned four resonant modes in the original elliptical cavity. Table 2 exhibits all dimensions of the proposed hepta-mode SIW elliptical CBSA. The simulated E-field distributions of the hepta-mode antenna are depicted in Figs. 10 (a)-(g), which are regarded as half quasi-TM<sub>010</sub> mode at 9.95 GHz, odd half degenerate quasi-TM<sub>110</sub> mode at 10.18 GHz, odd quasi-TM<sub>110</sub> mode at 10.61 GHz, even half degenerate quasi-TM<sub>110</sub> mode at

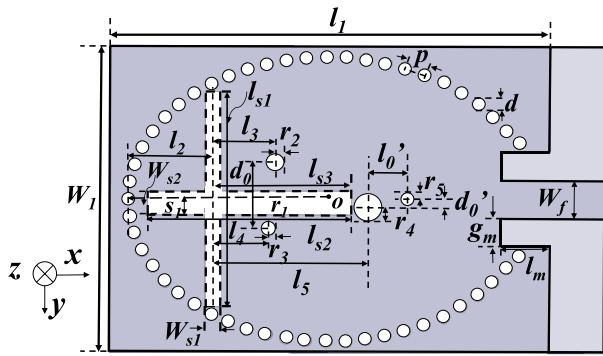


FIGURE 9. Geometry of the proposed hepta-mode SIW elliptical CBSA.

TABLE 2. Dimension of the proposed hepta-mode SIW elliptical CBSA.

Parameters	$l_1$	$l_2$	$l_3$	$l_4$	$l_5$
Values/mm	36.0	6.87	5.13	4.63	12.73
Parameters	$l_{s1}$	$l_{s2}$	$l_{s3}$	$l_0'$	$l_m$
Values/mm	17.5	16.7	11.33	3.2	4.0
Parameters	$w_1$	$w_{s1}$	$w_{s2}$	$w_f$	$d_0$
Values/mm	25.0	1.26	2.0	3.1	5.4
Parameters	$d_0'$	$r_1$	$r_2$	$r_3$	$r_4$
Values/mm	0.7	16.5	0.7	0.55	1.1
Parameters	$r_5$	$s_1$	$g_m$	$d$	$p$
Values/mm	0.5	0.3	2.35	1.0	1.4

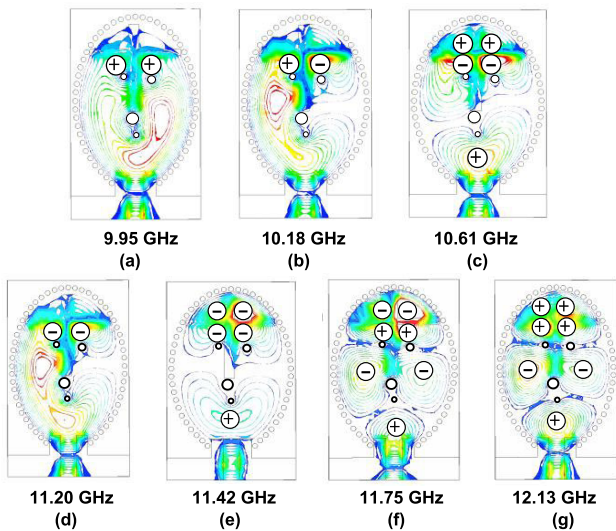


FIGURE 10. E-field distributions in the hepta-mode SIW elliptical CBSA. (a) half quasi-TM<sub>010</sub> mode, (b) odd half degenerate quasi-TM<sub>110</sub> mode, (c) odd quasi-TM<sub>110</sub> mode, (d) even half degenerate quasi-TM<sub>110</sub> mode, (e) even quasi-TM<sub>110</sub> mode, (f) odd quasi-TM<sub>210</sub> mode, (g) even quasi-TM<sub>210</sub> mode.

11.20 GHz, even quasi-TM<sub>110</sub> mode at 11.42 GHz, and odd- and even- quasi-TM<sub>210</sub> modes at 11.75 and 12.13 GHz, respectively. It is clear that all the seven resonant modes are sufficiently separated from others, without merging into any hybrid mode as reported in [14].

Likewise, Fig. 11 shows the design procedure for the generation of the seven resonant modes by using the variation

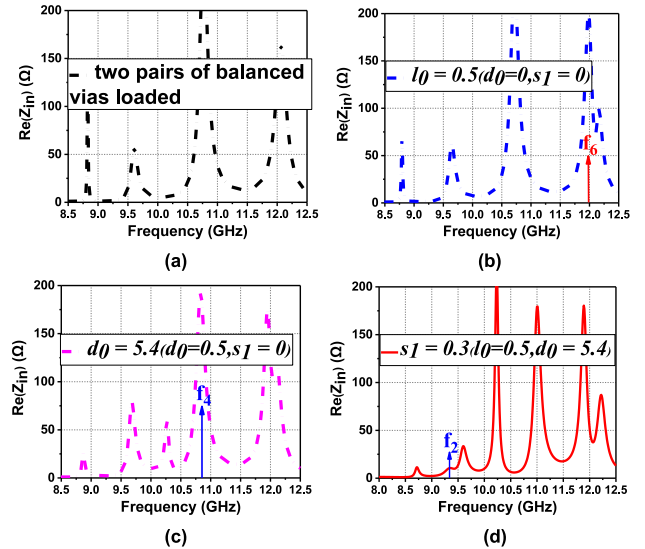


FIGURE 11. Simulated input resistance of the hepta-mode antenna with varying values for the parameters of the upper two shorting vias and the longitude slot (along x-axis). (a) two pairs of balanced vias loaded, (b) the relative offset  $l_0$  along x-axis, (c) the relative offset  $d_0$  along y-axis, (d) the movement  $s_1$  along y-axis.(unit: mm).

of the input resistance curves. The concrete design process of hepta-mode antenna is similarly summarized as follows: 1) repeating the design process of SIW elliptical cavity and the cross-shaped slot to generate the conventional tri-mode resonance as used in penta-mode CBSA; 2) Design of the unbalanced shorting vias: first, putting two pairs of balanced shorting vias into the elliptical cavity to shift upward the resonant frequencies of the half quasi-TM<sub>010</sub> mode and the odd- and even- quasi-TM<sub>110</sub> modes, and meanwhile introduce the even quasi-TM<sub>210</sub> mode as plotted in Fig. 11 (a). Second, offsetting the upper two vias along x-axis with the parameter  $l_0 = l_3 - l_4$  to excite the odd quasi-TM<sub>210</sub> mode as shown in Fig. 11 (b). Third, setting another offset between the upper two shorting vias along the y-axis with the parameter  $d_0$  and movement  $s_1$  to provide a further perturbation for exciting the even- and odd- half degenerate quasi-TM<sub>110</sub> modes, respectively, as observed in Fig. 11 (c) and (d). So far, the required seven resonant modes have been excited completely. The location and radius of the lower two shorting vias can be tuned as needed to achieve the best impedance match performance. The simulated and measured  $S$ -parameters of the proposed hepta-mode antenna are presented in Fig. 12, and the measured impedance bandwidth is 22.7% (9.75–12.25 GHz).

#### IV. RESULTS AND DISCUSSION

Fig. 13 illustrates two prototypes of the penta- and the hepta-resonance antennas, which are fabricated on a single-layer Taconic TLY substrate ( $\epsilon_r = 2.2$ , and  $\tan \delta = 0.0009$ ) with thickness of  $h = 1$  mm. The measured impedance bandwidth is 21.8% and 22.7%, respectively, as shown in Figs. 8 and 12. Fig. 14 displays the measured and simulated radiation patterns of these two types of antennas. The slight differences between the measured and simulated reflection coefficients

**TABLE 3.** Comparisons of the proposed antennas with previously published SIW rectangular CBSAs.

Ref.	Antennas	Fre. (GHz)	Dimension( $\lambda_0^3$ )	Impedance BW	Peak Gain (dBi)	Radiation Efficiency	Resonant modes
[4]	SIW rectangular CBSA	10	0.59×0.59×0.02	1.7%	5.4	> 75%	1
[5]	SIW rectangular CBSA	10	0.59×0.41×0.02	6.3%	6.0	> 81%*	2
[6]	SIW rectangular CBSA	10	0.59×0.53×0.03	9.4%	5.0	> 92%	2
[8]	SIW rectangular CBSA	28	0.58×0.86×0.05	16.7%	10.0	> 91%	3
[13]	SIW rectangular CBSA	10	0.63×0.77×0.03	15.2%	4.8	> 83%	3
		10	0.63×1.07×0.03	17.5%	7.3	> 84%	4
[14]	SIW rectangular CBSA	10	0.63×0.77×0.03	20.0%	4.9	> 86%*	4
		10	0.63×1.07×0.03	20.8%	5.7	> 84%*	5
This work	SIW elliptical CBSA	10	0.70×0.93×0.03	21.8%	7.0	> 92%	5
		10	0.77×1.10×0.03	22.7%	7.4	> 84%	7

\*: The radiation efficiency was measured, the other were simulated.

$\lambda_0$ : The wavelength of center frequency in the free space.

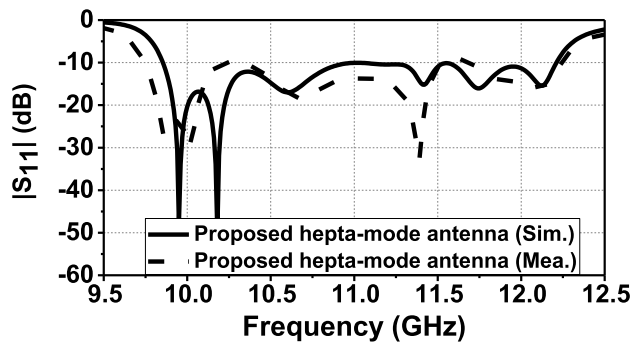


**FIGURE 12.** Measured reflection coefficient compared with the simulated results.

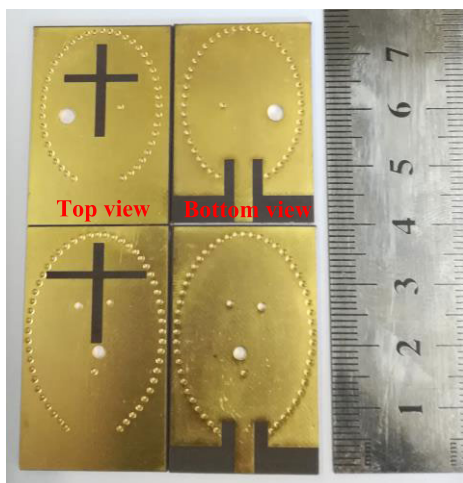


**FIGURE 13.** Photographs of two types of the proposed wideband SIW elliptical CBSAs.

are attributed to the fabrication tolerance and the coaxial connector, and the parasitic radiation from the connector further contributes to ripples appearing in the radiation patterns measured in the xoz-plane. The radiation efficiency and gain of the antennas are depicted in Fig. 15. The simulated radiation efficiency has a peak value of 97.2% and 95.6%, and the measured peak gain is 7.0 dBi and 7.4 dBi, respectively, both of which have a maximum gain variation within 2 dB. The gain fluctuation at high frequency is due to the alternating

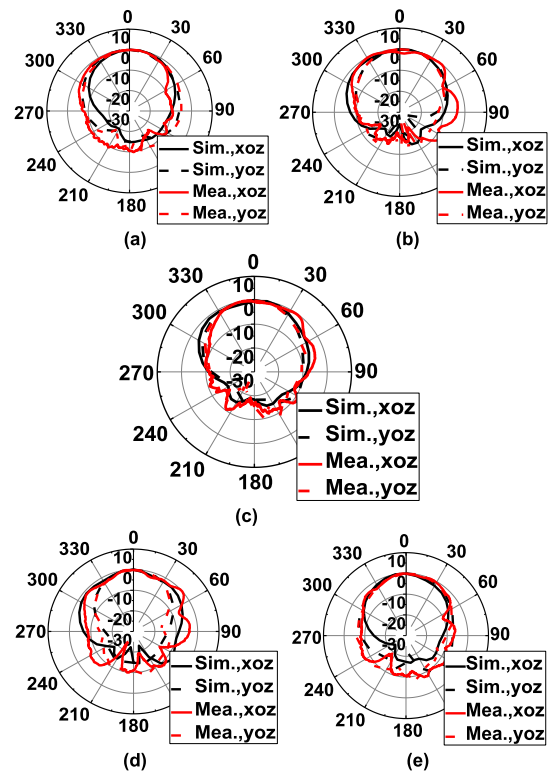


**FIGURE 14.** Simulated and measured radiation patterns of the penta-mode SIW elliptical CBSA at (a) 9.3 GHz and (b) 10.1 GHz, and the hepta-mode SIW elliptical CBSA at (c) 10 GHz, (d) 11 GHz, and (e) 12 GHz.

variation of in-and out-phase, which results in the small concaves on the gain and radiation efficiency curves.

Table 3 gives a comparison among the proposed penta- and hepta-resonance SIW elliptical CBSAs with other previously reported SIW rectangular CBSAs. As can be seen that these two types of proposed SIW elliptical CBSAs occupy the prominent bandwidths as well as a high radiation efficiency. Moreover, it is worth pointing out that the introduced both five and seven resonant modes in the elliptical cavity are generated completely, and neither hybrid modes nor mode merging appears when comparing previous works which use the rectangular cavity in [14]. The successful generation of five and seven modes contributes to a wider operating bandwidth

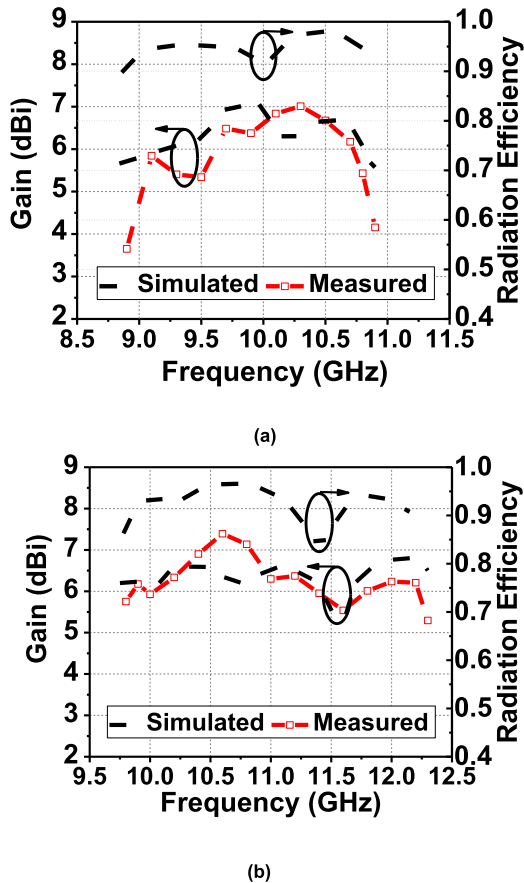


**FIGURE 15.** Gain and radiation efficiency of the proposed SIW elliptical CBSA. (a) Penta-mode, (b) Hepta-mode.

as expected. In addition, although prototypes are fabricated and measured at X-band, the presented design guidelines are independent of operating frequency, which is that the shape of the elliptical cavity is only determined by its axial ratio  $k$ , and the placement of cross-shape slot and shorting vias are mainly associated with E-field distributions of the resonant modes. Therefore, the proposed SIW CBSAs, by tuning their absolute geometrical size, can be theoretically implemented at any targeted frequency band, including millimeter-wave band, which will be studied in future work.

## V. CONCLUSION

For X-band wideband wireless applications, two types of SIW elliptical CBSAs have been designed. The proposed penta- and hepta-resonance CBSAs exhibit a low profile of  $0.03\lambda_0$ , flexible tuning ability, and wide impedance bandwidth. For the penta-mode antenna, a wide bandwidth is obtained with the assistance of a cross-shaped slot and a pair of unbalanced shorting vias. As for the hepta-mode antenna, a wider bandwidth is accomplished through adding another pair of unbalanced shorting vias. To verify the design principles, prototypes of these SIW elliptical CBSAs have been fabricated and measured. Measured results show that the penta- and hepta-resonance antennas possess broad impedance bandwidths of 21.8% and 22.7%, respectively.

## REFERENCES

- [1] K. K. Sadasivuni, J.-J. Cabibihan, D. Ponnamma, M. A. S. Al-Maadeed, and J. Kim, *Biopolymer Composites in Electronics*. New York, NY, USA: Elsevier, 2016.
- [2] D. M. Pozar, *Microwave Engineering*. Hoboken, NJ, USA: Wiley, 2009.
- [3] C. Locker, T. Vaupel, and T. F. Eibert, "Radiation efficient unidirectional low-profile slot antenna elements for X-band application," *IEEE Trans. Antennas Propag.*, vol. 53, no. 8, pp. 2765–2768, Aug. 2005.
- [4] G. Qing Luo, Z. Fang Hu, L. Xi Dong, and L. Ling Sun, "Planar slot antenna backed by substrate integrated waveguide cavity," *IEEE Antennas Wireless Propag. Lett.*, vol. 7, pp. 236–239, 2008.
- [5] G. Q. Luo, Z. F. Hu, W. J. Li, X. H. Zhang, L. L. Sun, and J. F. Zheng, "Bandwidth-enhanced low-profile cavity-backed slot antenna by using hybrid SIW cavity modes," *IEEE Trans. Antennas Propag.*, vol. 60, no. 4, pp. 1698–1704, Apr. 2012.
- [6] S. Mukherjee, A. Biswas, and K. V. Srivastava, "Broadband substrate integrated waveguide cavity-backed bow-tie slot antenna," *IEEE Antennas Wireless Propag. Lett.*, vol. 13, pp. 1152–1155, 2014.
- [7] S. Mukherjee, A. Biswas, and K. V. Srivastava, "Substrate integrated waveguide cavity-backed dumbbell-shaped slot antenna for dual-frequency applications," *IEEE Antennas Wireless Propag. Lett.*, vol. 14, pp. 1314–1317, 2015.
- [8] P. N. Choubey, W. Hong, Z.-C. Hao, P. Chen, T.-V. Duong, and J. Mei, "A wideband dual-mode SIW cavity-backed triangular-complementary-split-ring-slot (TCSRS) antenna," *IEEE Trans. Antennas Propag.*, vol. 64, no. 6, pp. 2541–2545, Jun. 2016.
- [9] G. Q. Luo, Z. F. Hu, Y. Liang, L. Y. Yu, and L. L. Sun, "Development of low profile cavity backed crossed slot antennas for planar integration," *IEEE Trans. Antennas Propag.*, vol. 57, no. 10, pp. 2972–2979, Oct. 2009.
- [10] T. Deckmyn, S. Agneessens, A. C. F. Reniers, A. B. Smolders, M. Cauwe, D. V. Ginste, and H. Rogier, "A novel 60 GHz wideband coupled half-mode/quarter-mode substrate integrated waveguide antenna," *IEEE Trans. Antennas Propag.*, vol. 65, no. 12, pp. 6915–6926, Dec. 2017.
- [11] T. Deckmyn, M. Cauwe, D. V. Ginste, H. Rogier, and S. Agneessens, "Dual-band (28,38) GHz coupled quarter-mode substrate-integrated waveguide antenna array for next-generation wireless systems," *IEEE Trans. Antennas Propag.*, vol. 67, no. 4, pp. 2405–2412, Apr. 2019.
- [12] B.-J. Niu and J.-H. Tan, "Bandwidth enhancement of low-profile SIW cavity antenna using fraction modes," *Electron. Lett.*, vol. 55, no. 5, pp. 233–234, Mar. 2019.
- [13] Y. Shi, J. Liu, and Y. Long, "Wideband triple- and quad-resonance substrate integrated waveguide cavity-backed slot antennas with shorting vias," *IEEE Trans. Antennas Propag.*, vol. 65, no. 11, pp. 5768–5775, Nov. 2017.
- [14] Q. Wu, J. Yin, C. Yu, H. Wang, and W. Hong, "Broadband planar SIW cavity-backed slot antennas aided by unbalanced shorting vias," *IEEE Antennas Wireless Propag. Lett.*, vol. 18, no. 2, pp. 363–367, Feb. 2019.
- [15] W. Han, F. Yang, J. Ouyang, and P. Yang, "Low-cost wideband and high-gain slotted cavity antenna using high-order modes for millimeter-wave application," *IEEE Trans. Antennas Propag.*, vol. 63, no. 11, pp. 4624–4631, Nov. 2015.
- [16] S. Mukherjee, A. Biswas, and K. V. Srivastava, "Substrate integrated waveguide cavity backed slot antenna for dual-frequency application," in *Proc. 44th Eur. Microw. Conf.*, Oct. 2014, pp. 57–60.
- [17] S. Mukherjee, A. Biswas, and K. V. Srivastava, "Substrate integrated waveguide cavity backed slot antenna for dual-frequency application," in *Proc. 44th Eur. Microw. Conf.*, Oct. 2014, pp. 7–11.
- [18] T. Yang Yang, W. Hong, and Y. Zhang, "Wideband millimeter-wave substrate integrated waveguide cavity-backed rectangular patch antenna," *IEEE Antennas Wireless Propag. Lett.*, vol. 13, pp. 205–208, 2014.
- [19] K. Fan, Z.-C. Hao, and Q. Yuan, "A low-profile wideband substrate-integrated waveguide cavity-backed E-shaped patch antenna for the Q-LINKPAN applications," *IEEE Trans. Antennas Propag.*, vol. 65, no. 11, pp. 5667–5676, Nov. 2017.
- [20] G. Qing Luo and L. Ling Sun, "Circularly polarized antenna based on dual-mode circular SIW cavity," in *Proc. Int. Conf. Microw. Millim. Wave Technol.*, Apr. 2008, pp. 1077–1079.
- [21] D.-Y. Kim, J. W. Lee, T. K. Lee, and C. S. Cho, "Design of SIW cavity-backed circular-polarized antennas using two different feeding transitions," *IEEE Trans. Antennas Propag.*, vol. 59, no. 4, pp. 1398–1403, Apr. 2011.
- [22] E.-Y. Jung, J. W. Lee, T. K. Lee, and W.-K. Lee, "SIW-based array antennas with sequential feeding for X-band satellite communication," *IEEE Trans. Antennas Propag.*, vol. 60, no. 8, pp. 3632–3639, Aug. 2012.

- [23] Q. Wu, H. Wang, C. Yu, and W. Hong, "Low-profile circularly polarized cavity-backed antennas using SIW techniques," *IEEE Trans. Antennas Propag.*, vol. 64, no. 7, pp. 2832–2839, Jul. 2016.
- [24] Q. Wu, J. Yin, C. Yu, H. Wang, and W. Hong, "Low-profile millimeter-wave SIW cavity-backed dual-band circularly polarized antenna," *IEEE Trans. Antennas Propag.*, vol. 65, no. 12, pp. 7310–7315, Dec. 2017.
- [25] T. Hong, Z. Zhao, W. Jiang, S. Xia, Y. Liu, and S. Gong, "Dual-band SIW cavity-backed slot array using TM<sub>020</sub> and TM<sub>120</sub> modes for 5G applications," *IEEE Trans. Antennas Propag.*, vol. 67, no. 5, pp. 3490–3495, May 2019.
- [26] J. Yan, F. Xu, K. Cao, and J. Qian, "Planar slot antenna based on triangle substrate integrated waveguide cavity," in *Proc. IEEE Int. Conf. Ubiquitous Wireless Broadband (ICUBW)*, Oct. 2016, pp. 1–3.
- [27] G. Zhang and Z. Xu, "Development of circularly polarized antennas based on dual-mode hexagonal SIW cavity," in *Proc. 15th Int. Conf. Electron. Packag. Technol.*, May 2014, pp. 1283–1286.
- [28] L. Accatino, G. Bertin, and M. Mongiardo, "Elliptical cavity resonators for dual-mode narrow-band filters," *IEEE Trans. Microw. Theory Techn.*, vol. 45, no. 12, pp. 2393–2401, Dec. 1997.
- [29] J. G. Kretschmar, "Wave propagation in hollow conducting elliptical waveguides," *IEEE Trans. Microw. Theory Techn.*, vol. 18, no. 9, pp. 547–554, Sep. 1970.



**LEI XIANG** was born in Kunming, Yunnan, China, in 1995. She received the B.S. degree in electronics and information engineering from Xidian University, Xi'an, China, in 2018. She is currently pursuing the Ph.D. degree in electro-magnetic field and microwave technology with the State Key Laboratory of Millimeter Waves, Southeast University, Nanjing, China.

Her current research interests include antenna design and wireless communication systems.



**YAN ZHANG** (Member, IEEE) received the B.Eng. degree in information engineering and the Ph.D. degree in electrical engineering from Southeast University (SEU), Nanjing, China, in 2006 and 2012, respectively.

From January 2009 to July 2009, he was a Research Engineer with the Institute for Infocomm Research (I2R), Agency for Science, Technology, and Research (A\* STAR), Singapore. From November 2009 to December 2010, he was a Visiting Scholar with the Electromagnetic Communication Laboratory, Pennsylvania State University. Since December 2011, he has been a Researcher with the State Key Laboratory of Millimeter Waves, SEU. He has published over 20 peer-viewed journal articles. He holds 14 granted and filed patents. His research interests include millimeter-wave and terahertz antennas, planar transmission line techniques and filters, RF and antenna design for satellite communication.

Dr. Zhang was a recipient of the Best Student Paper Award of the 2008 International Conference on Microwave and Millimeter Wave Technology (ICMMT'2008) and the 2013 International Symposium on Antennas and Propagation (ISAP'2013). He serves as a Reviewer for several journals, including the IEEE TRANSACTIONS ON ANTENNAS AND PROPAGATION, the IEEE ANTENNA AND PROPAGATION LETTERS, the IEEE MICROWAVE WIRELESS COMPONENT LETTERS, *PIER*, and so on.



**YINGRUI YU** (Graduate Student Member, IEEE) was born in Nanjing, China, in 1992. He received the B.S. degree in communication engineering from the Nanjing University of Science and Technology (NJUST), Nanjing, in 2014. He is currently pursuing the Ph.D. degree in microwave technology with the State Key Laboratory of Millimeter Waves, Southeast University, Nanjing.

From 2018 to 2019, he was an Honorary Associate with the Department of Electrical and Computer Engineering (ECE), University of Wisconsin–Madison, Madison, WI, USA. He has authored several journal articles in the IEEE TRANSACTIONS ON ANTENNAS AND PROPAGATION. His current research interests include antenna array theory and design, millimeter-wave radar, and communication systems.

Mr. Yu was a recipient of the Scholarship from the China Scholarship Council. From 2011 to 2013, he was also thrice awarded the National Scholarship for Undergraduate Students issued by the Ministry of Education of China. He serves as a Reviewer for IEEE ACCESS, the *Electronics Letters*, and the *AEÜ- International Journal of Electronics and Communications*.



**WEI HONG** (Fellow, IEEE) received the B.S. degree in radio engineering from the University of Information Engineering, Zhengzhou, China, in 1982, and the M.S. and Ph.D. degrees in radio engineering from Southeast University, Nanjing, China, in 1985 and 1988, respectively.

Since 1988, he has been with the State Key Laboratory of Millimeter Waves, Southeast University. Since 2003, he has been the Director of the Laboratory. He was a short-term Visiting Scholar with the University of California at Berkeley and Santa Cruz, in 1993, 1995, 1996, 1997, and 1998, respectively. He is currently a Professor with the School of Information Science and Engineering, Southeast University. He has been engaged in numerical methods for electromagnetic problems, millimeter-wave theory and technology, antennas, RF technology for wireless communications, and so on. He has authored or coauthored over 300 technical publications and two books.

Dr. Hong is a Fellow of CIE. He was an elected IEEE MTT-S AdCom Member From 2014 to 2016. He twice received the National Natural Prizes, thrice the First-Class Science and Technology Progress Prizes issued by the Ministry of Education of China and Jiangsu Province Government, the Foundations for China Distinguished Young Investigators and for Innovation Group issued by NSF of China, and so on. He is also the Chair of the IEEE MTT-S/AP-S/EMC-S Joint Nanjing Chapter. He is the Vice President of the CIE Microwave Society and Antenna Society. From 2007 to 2010, he served as an Associate Editor for the IEEE TRANSACTIONS ON MICROWAVE THEORY AND TECHNIQUES.

...